Meteorological Model Performance for Annual 2007 Simulations

EPA-454/R-11-007
October 2011

Meteorological Model Performance for Annual 2007 Simulations

U.S. Environmental Protection Agency
Office of Air Quality Planning and Standards
Air Quality Assessment Division
Research Triangle Park, NC 27711

1. INTRODUCTION

The Weather Research and Forecasting model (WRF) has been applied for the entire year of 2007 to support future emissions and photochemical modeling applications. It is expected that these meteorological fields will be converted and used to support assessments of ozone, PM2.5, visibility, and a variety of toxics. Charts showing monthly precipitation relative to an area's climatic norm are shown in Appendix A for additional information about regional differences in meteorology in 2007 compared to the weather an area might typically experience.

The WRF model was applied to a 36 km continental United States scale domain (36US1) and a 12 km continental United States scale domain (12US1) for the entire year of 2007. Both model simulations were initialized directly from meteorological analysis data. The model parameterizations and options outlined in this document were chosen based on a series of sensitivity runs performed by U.S. Environmental Protection Agency Office of Research and Development that provided an optimal configuration based on temperature, mixing ratio, and wind field. All WRF simulations were done by Computer Sciences Corporation (CSC) under contract from the United States Environmental Protection Agency.

2 MODEL CONFIGURATION

2.1 Configuration of the 12US domain

Meteorological inputs are generated with version 3.1 of the Weather Research and Forecasting model (WRF), Advanced Research WRF (ARW) core (Skamarock, 2008). Important selected physics options include Pleim-Xiu land surface model, Asymmetric Convective Model version 2 planetary boundary layer scheme, Kain-Fritsh cumulus parameterization, Morrison double moment microphysics, RRTMG longwave, and RRTMG shortwave radiation scheme (Gilliam and Pleim, 2010).

The WRF model was initialized using the 12NAM analysis product provided by NCDC (http://nomads.ncdc.noaa.gov/data.php?name=access#hires_weather_datasets) and backfilled with 36 km AWIP/EDAS analysis (ds609.2) from NCAR (http://www.mmm.ucar.edu/mm5/mm5v3/data/free_data.html) where 12NAM is not available. Three dimensional analyses nudging for temperature and moisture is applied above the boundary layer only. Analysis nudging for the wind is applied above and below the boundary layer. The model is applied in blocks of 5 and a half days. Soil moisture and soil temperature are carried over from one 5.5 day block to the next using the **ipxwrf** program (Gilliam and Pleim, 2010). Landuse and land cover data are based on 2001 National Land Cover Data (http://www.mrlc.gov/nlcd2001.php) that is translated for use in WRF.

The 12US domain is shown in Figure 2.1. The domain is a lambert conformal projection centered at (-97, 40) with true latitudes at 33 and 45 degrees north. The domain contains 459 cells in the X direction and 299 cells in the Y direction. All cells are 12 km square. There are 34 layers resolving the vertical atmosphere up to 50 mb, the thinnest layers being nearest the surface to better resolve the variations in the planetary boundary layer.

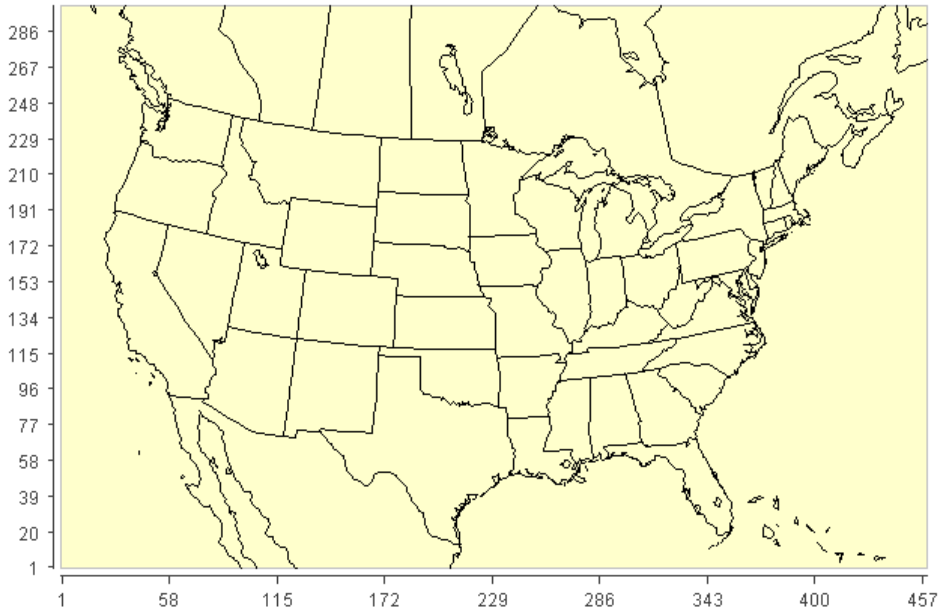

Figure 2.1 Map of WRF model domain: 12US

2.2 Configuration of the 36US domain

Meteorological inputs are generated with version 3.3 of the Weather Research and Forecasting model (WRF), Advanced Research WRF (ARW) core (Skamarock, 2008). Important selected physics options include Pleim-Xiu land surface model, Asymmetric Convective Model version 2 planetary boundary layer scheme, Kain-Fritsh cumulus parameterization, Morrison double moment microphysics, RRTMG longwave, and RRTMG shortwave radiation scheme (Gilliam and Pleim, 2010).

The WRF model was initialized using the 12NAM analysis product provided by NCDC (http://nomads.ncdc.noaa.gov/data.php?name=access#hires_weather_datasets) and backfilled with 36 km AWIP/EDAS analysis (ds609.2) from NCAR (http://www.mmm.ucar.edu/mm5/mm5v3/data/free_data.html) where 12NAM is not available. Three dimensional analyses nudging for temperature, wind field, and moisture is applied above the boundary layer only. The model is applied in blocks of 5 and a half days. Soil moisture and soil temperature are carried over from one 5.5 day block to the next using the **ipxwrf** program (Gilliam and Pleim, 2010). Landuse and land cover data are based on U.S. Geological Survey (USGS) data that is distributed with the WRF model.

The 36US domain is shown in Figure 2.2. The domain is a lambert conformal projection centered at (-97, 40) with true latitudes at 33 and 45 degrees north. The domain contains 148 cells in the X direction and 112 cells in the Y direction. All cells are 36 km square. There are 34 layers resolving the vertical atmosphere up to 50 mb, the thinnest layers being nearest the surface to better resolve the variations in the planetary boundary layer.

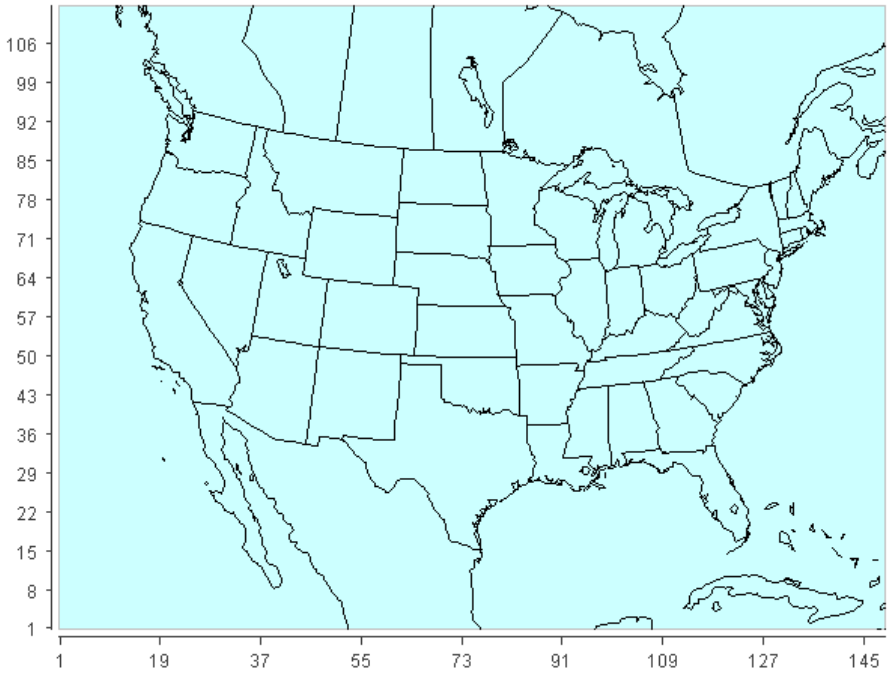

Figure 2.2 Map of WRF model domain: 36US

2.3 WRF Conversion to Photochemical Model Inputs

CMAQ-ready meteorological input files were prepared using the Meteorology-Chemistry Interface Processor (MCIP) package (Otte and Pleim, 2010). The code is available at www.cmascenter.org. MCIP v4.0 was used for the 36US1 domain and version 3.6 of the MCIP processor was used to generate CMAQ ready meteorological files for the 12US1 domain. CAMx meteorological input files for both 36US1 and 12US1 were prepared using WRFCAMx version 3.1 (ENVIRON, 2008). The WRFCAMx processor is available at www.camx.com.

Table 2.3 shows the vertical layer structure used in WRF and the layer collapsing approach to generated photochemical model (PCM) meteorological inputs. The photochemical models resolve the vertical atmosphere with 24 layers, preserving greater resolution in the planetary boundary layer to better resolve the diurnal changes in PBL heights.

Table 2.3. Vertical layer structure of WRF simulations.

Height (m)	Pressure (mb)	WRF	Depth (m)	PCM	Depth (m)
17,145	50	34	2,655	24	4,552
14,490	95	33	1,896		
12,593	140	32	1,499	23	2,749
11,094	185	31	1,250		
9,844	230	30	1,078	22	2,029
8,766	275	29	951		
7,815	320	28	853	21	1,627
6,962	365	27	775		
6,188	410	26	711	20	1,368
5,477	455	25	657		
4,820	500	24	612	19	1,185
4,208	545	23	573		
3,635	590	22	539	18	539
3,095	635	21	509	17	509
2,586	680	20	388	16	388
2,198	716	19	281	15	281
1,917	743	18	273	14	273
1,644	770	17	178	13	178
1,466	788	16	174	12	174
1,292	806	15	171	11	171
1,121	824	14	168	10	168
952	842	13	165	9	165
787	860	12	82	8	163
705	869	11	81		
624	878	10	80	7	160
544	887	9	80		
465	896	8	79	6	157
386	905	7	78		
307	914	6	78	5	78
230	923	5	77	4	77
153	932	4	38	3	76
114	937	3	38		
76	941	2	38	2	38
38	946	1	38	1	38

3 MODEL PERFORMANCE DESCRIPTION

One of the objectives of this evaluation is to determine if the meteorological model output fields represent a reasonable approximation of the actual meteorology that occurred during the modeling period. A second objective is to identify and quantify the existing biases and errors of the meteorological predictions in order to allow for a downstream assessment of how the air quality modeling results are affected by issues associated with the meteorological data. Performance results are presented to allow those using this data to determine the adequacy of the model simulation for their particular needs.

The observation database for temperature, wind speed, wind direction, and mixing ratio is based on measurements made at United States and Canada airports. The observation data (ds472) is available from NCAR (http://dss.ucar.edu/datasets/ds472.0). Monitors used for evaluation as part of the NCAR observation package are shown in Figure 3.1.

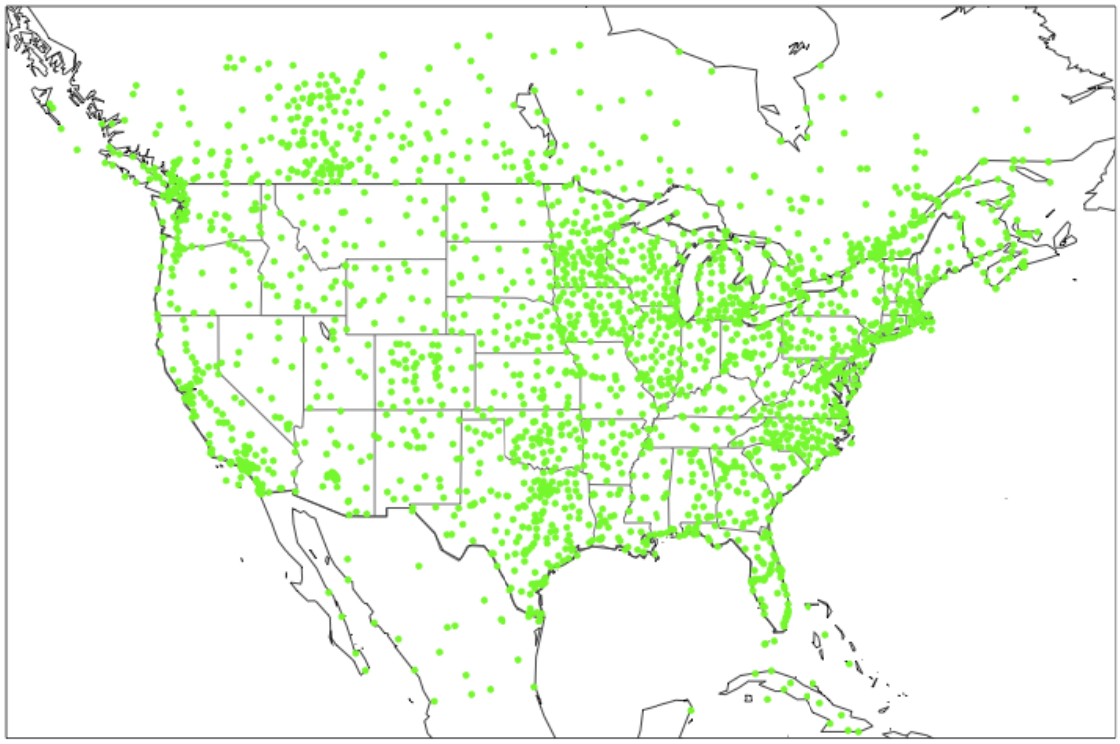

Figure 3.1 Stations used for model performance: ds472 network.

Rainfall analysis estimated by the PRISM model is approximately 2 to 4 km resolution and is compared to model estimates. The rainfall analysis data does not include any portion of Canada, Mexico, or anywhere off-shore of the United States (http://www.prism.oregonstate.edu). The rainfall analysis is reprojected to the modeling domain for direct qualitative comparison to model estimates.

Shortwave downward radiation measurements are taken at SURFRAD (http://www.srrb.noaa.gov/surfrad) and ISIS (http://www.srrb.noaa.gov/isis/index.html) monitor locations. The SURFRAD network consists of 7 sites and the ISIS network consists of 8 sites across the United States.

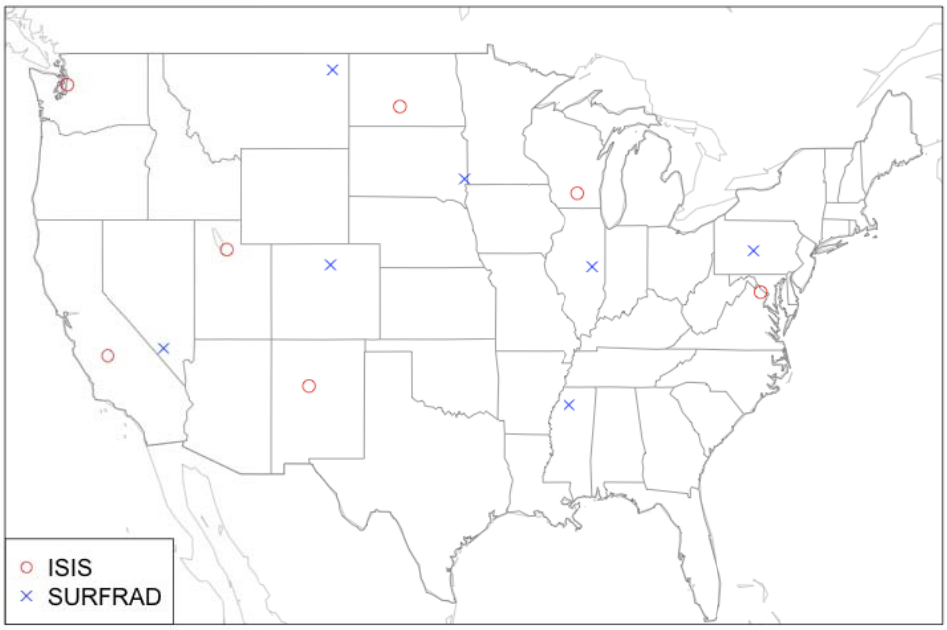

Figure 3.2 Stations used for model performance: SURFRAD and ISIS networks.

Model performance is described using quantitative metrics: mean bias, mean (gross) error, fractional bias, and fractional error (Boylan and Russell, 2006). These metrics are useful because they describe model performance in the measured units of the meteorological variable and as a normalized percentage. Since wind direction is reported in compass degrees estimating performance metrics is problematic since modeled and observed northerly winds may be similar but the difference would result in a very large "bias". Wind field displacement, or the difference in the **U** and **V** vectors between modeled (M) and observed (O) values, is used to assess wind vector performance (Equation 1). Performance is best when these metrics approach 0.

(1) Wind displacement (km) = $(\mathbf{U}_M - \mathbf{U}_O + \mathbf{V}_M - \mathbf{V}_O)$*(1 km/1000 m)*(3600 s/hr)*(1 hr)

Rainfall performance is examined qualitatively with side-by-side monthly total rainfall plots. The WRF model outputs predictions approximately 15 meters above the surface while observations are at 10 meters. WRF outputs near instantaneous values (90 second time step) as opposed to the values with longer averaging times taken at monitor stations. This should be considered when interpreting model performance metrics.

3.1 Wind Field

Wind speed estimates are compared to surface based measurements made at NCAR's ds472 network monitors for the 12US (Figure 3.1.1) and 36US (Figure 3.1.2) domains. Outliers are not plotted on these box plots to emphasize predominant features in model performance. The outer edges of the box represent the 25th and 75th percentiles and the edges of the whiskers represent the 10th and 90th percentiles of the distributions. These plots show the entire distribution of

hourly bias (model-observation) by month and by hour of the day. In addition, these Figures show other metrics including mean error, fractional bias, and fractional error.

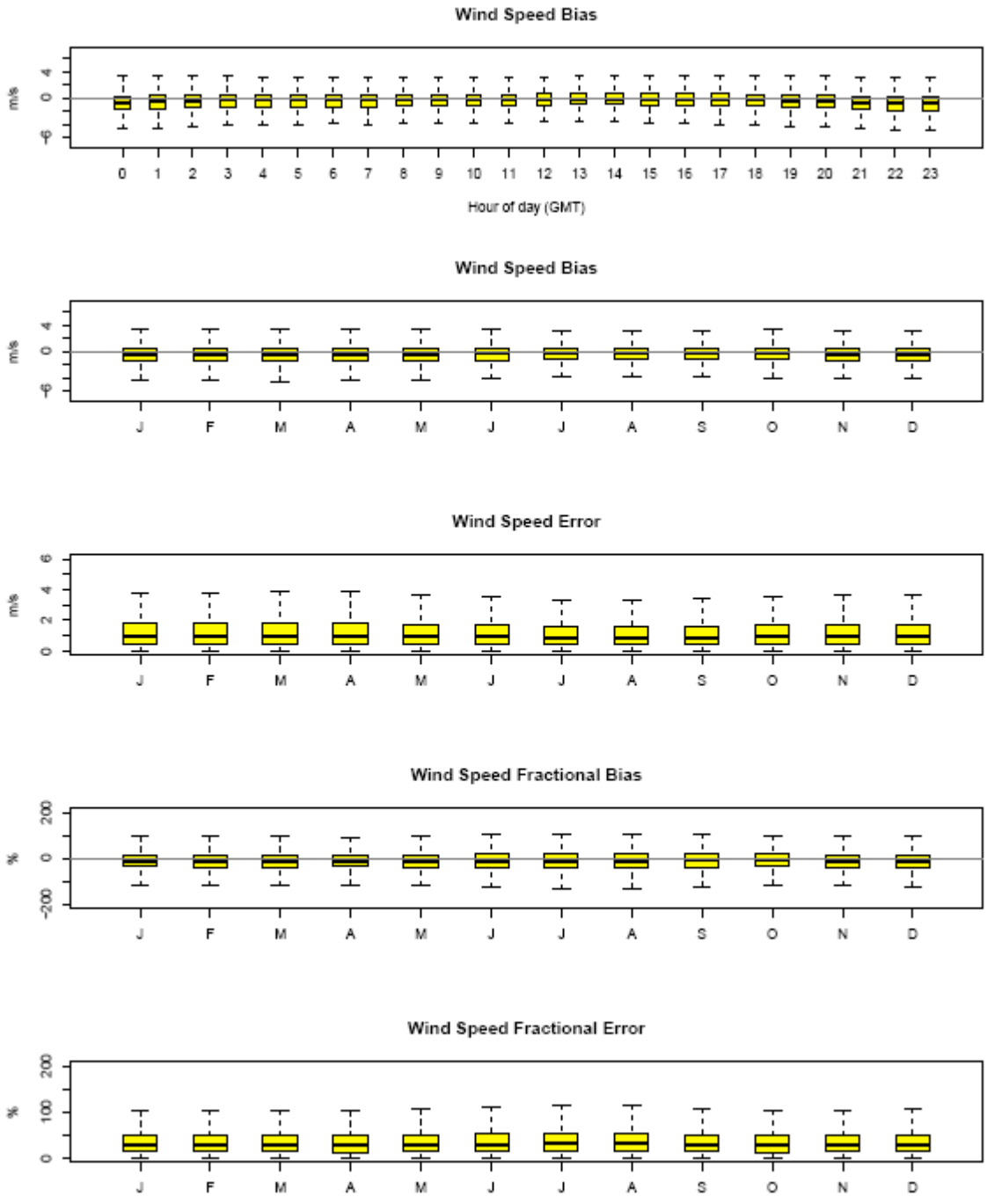

Figure 3.1.1. Distribution of hourly bias by hour and hourly bias, error, fractional bias, and fractional error by month. Metrics shown for 12US domain.

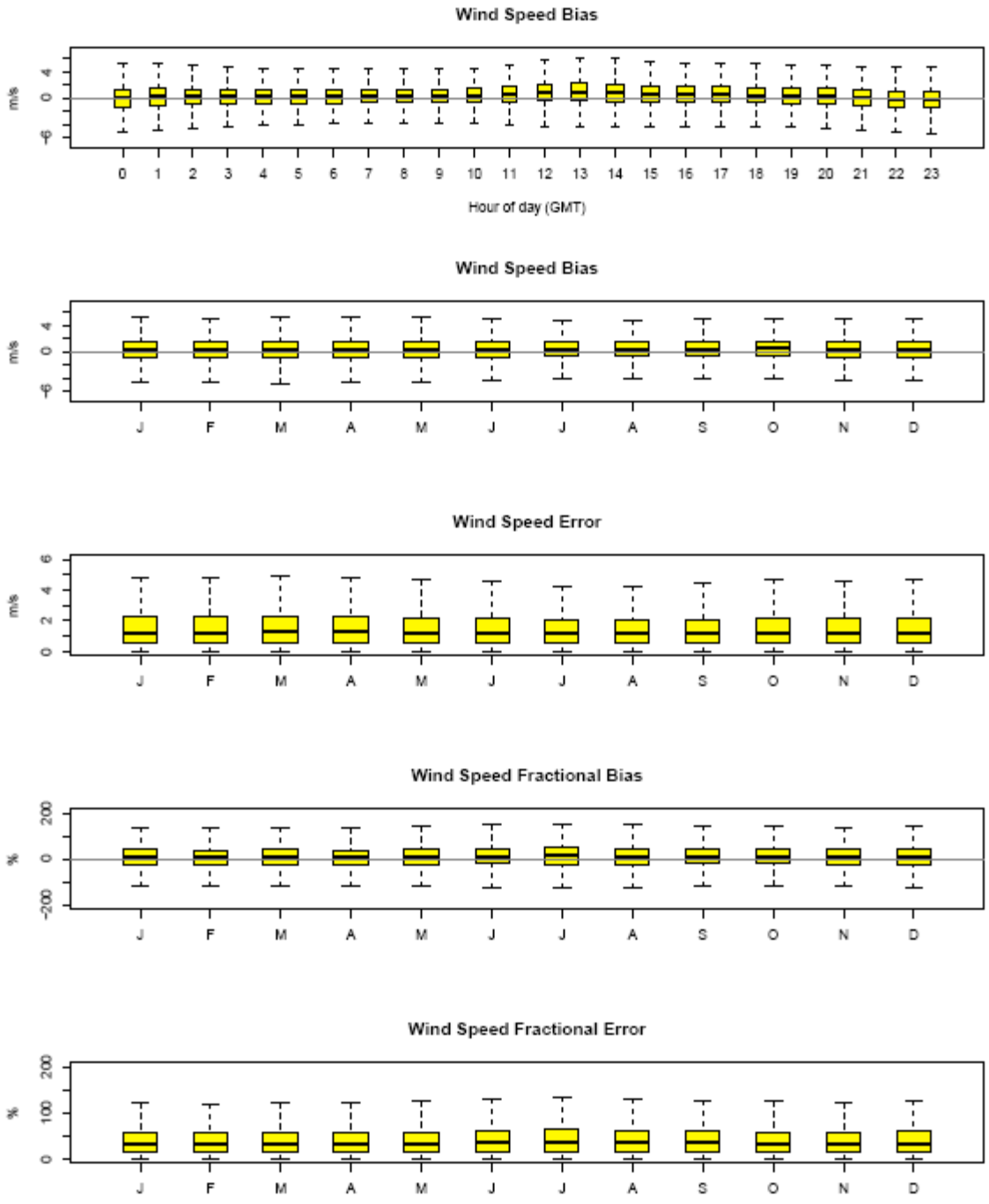

Figure 3.1.2. Distribution of hourly bias by hour and hourly bias, error, fractional bias, and fractional error by month. Metrics shown for 36US domain.

Wind vector displacement (km) is estimated at NCAR's ds472 network monitors for the 12US (Figure 3.1.3) and 36US (Figure 3.1.4) domains. Outliers are not plotted on these box plots to emphasize predominant features in model performance. The outer edges of the box represent the 25th and 75th percentiles and the edges of the whiskers represent the 10th and 90th percentiles of

the distributions. These plots show the entire distribution of hourly wind displacement by month and by hour of the day.

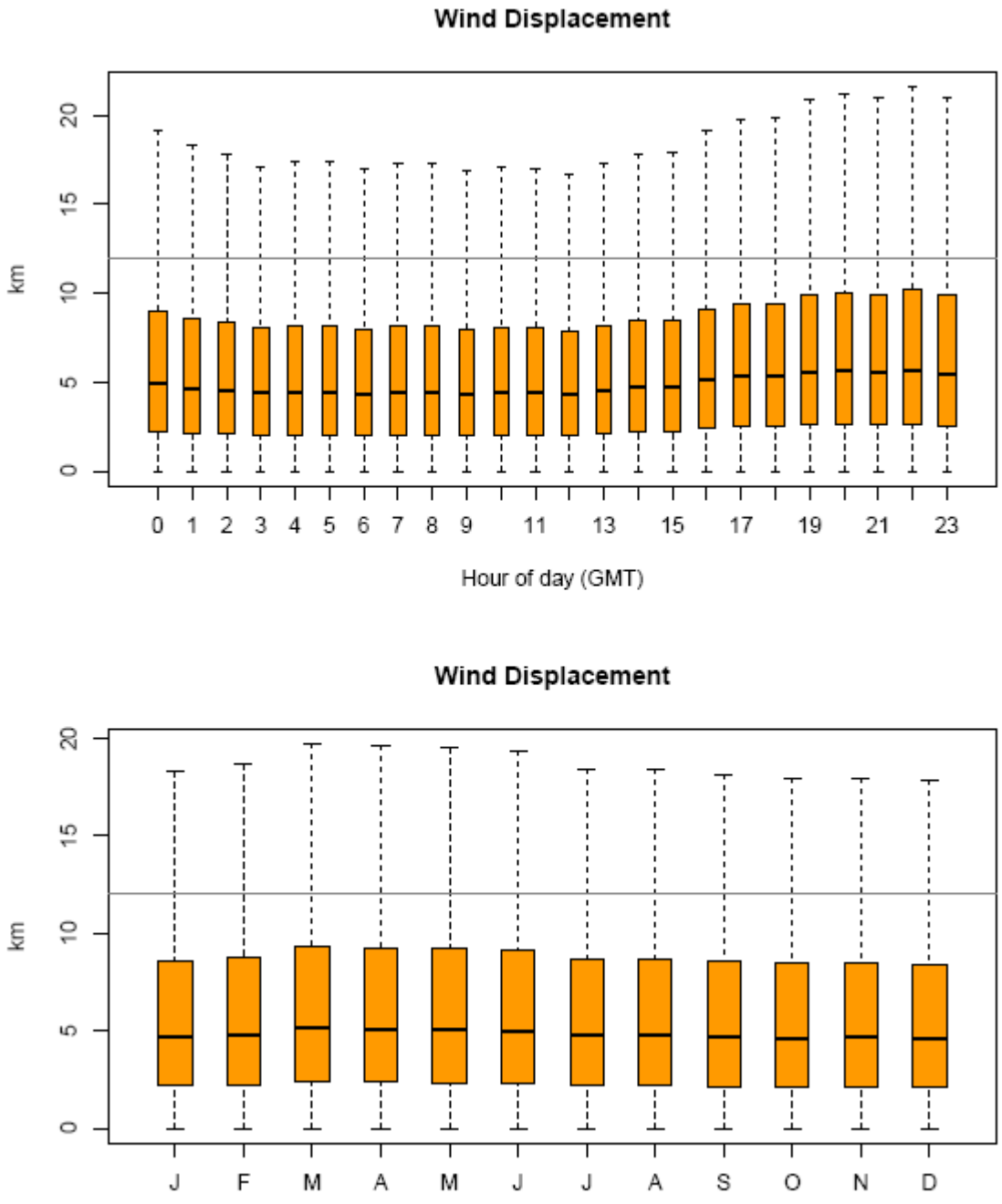

Figure 3.1.3. Distribution of hourly wind displacement by hour and month. Metrics shown for 12US domain.

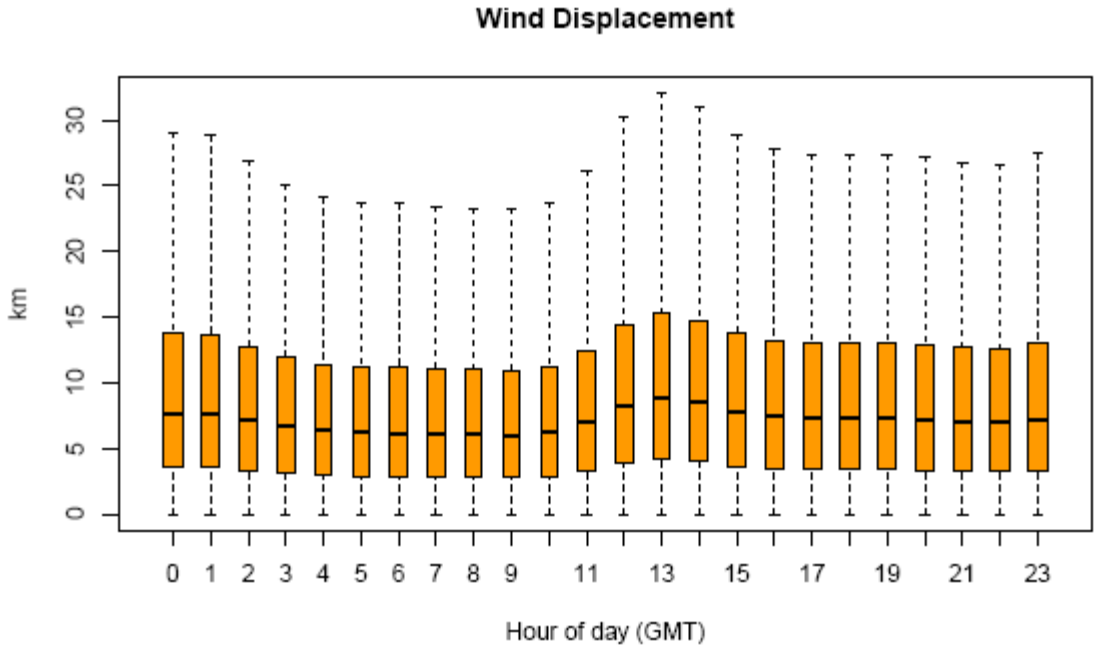

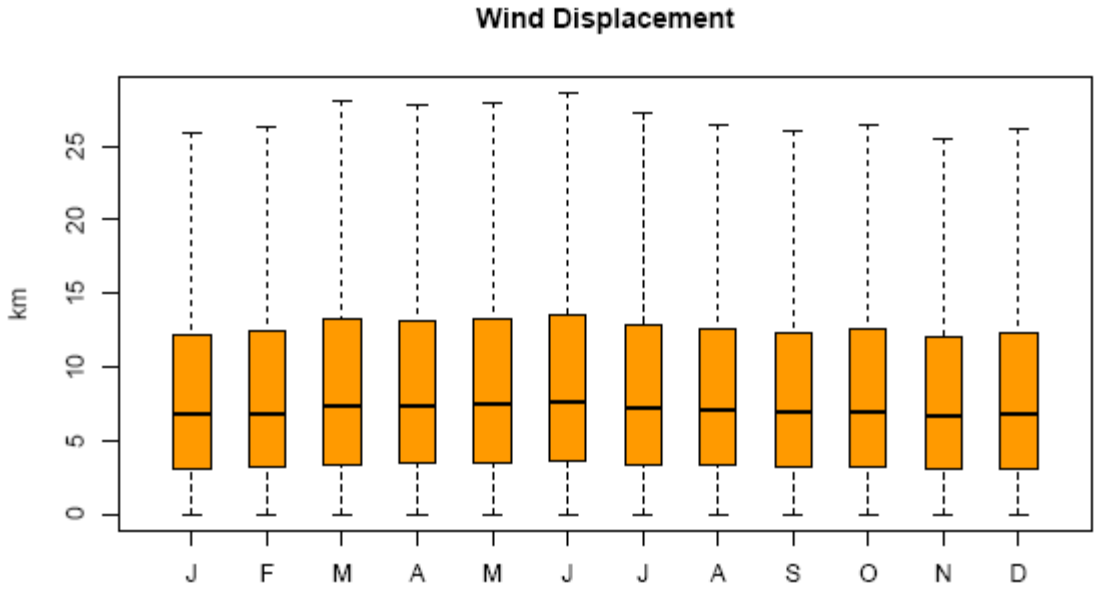

Figure 3.1.4. Distribution of hourly wind displacement by hour and month. Metrics shown for 36US domain.

3.2 Temperature

Temperature estimates are compared to surface based measurements made at NCAR's ds472 network monitors for the 12US (Figure 3.2.1) and 36US (Figure 3.2.2) domains. Outliers are not

plotted on these box plots to emphasize predominant features in model performance. The outer edges of the box represent the 25th and 75th percentiles and the edges of the whiskers represent the 10th and 90th percentiles of the distributions. These plots show the entire distribution of hourly bias (model-observation) by month and by hour of the day. In addition, these Figures show other metrics including mean error, fractional bias, and fractional error.

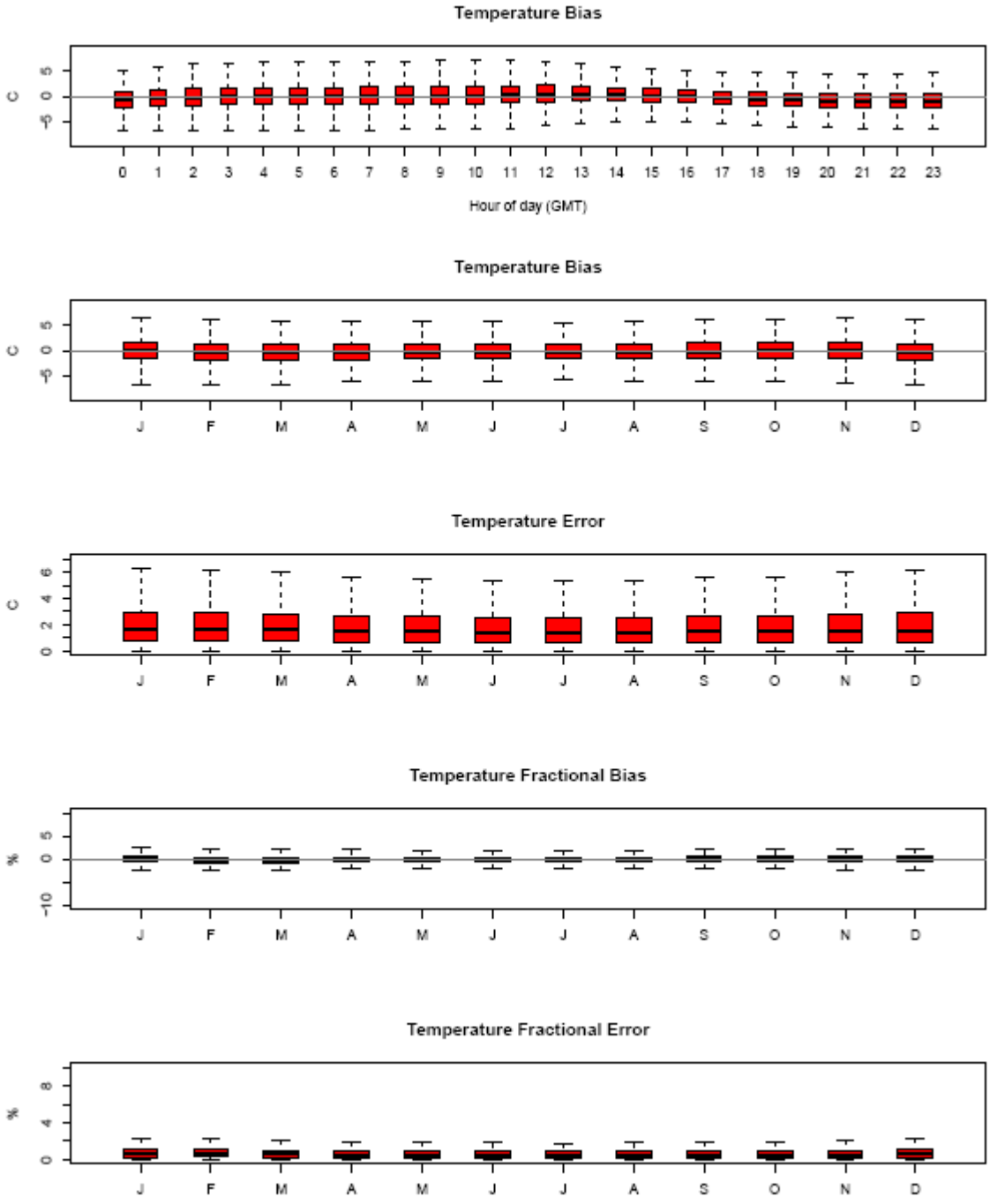

Figure 3.2.1. Distribution of hourly bias by hour and hourly bias, error, fractional bias, and fractional

error by month. Metrics shown for 12US domain.

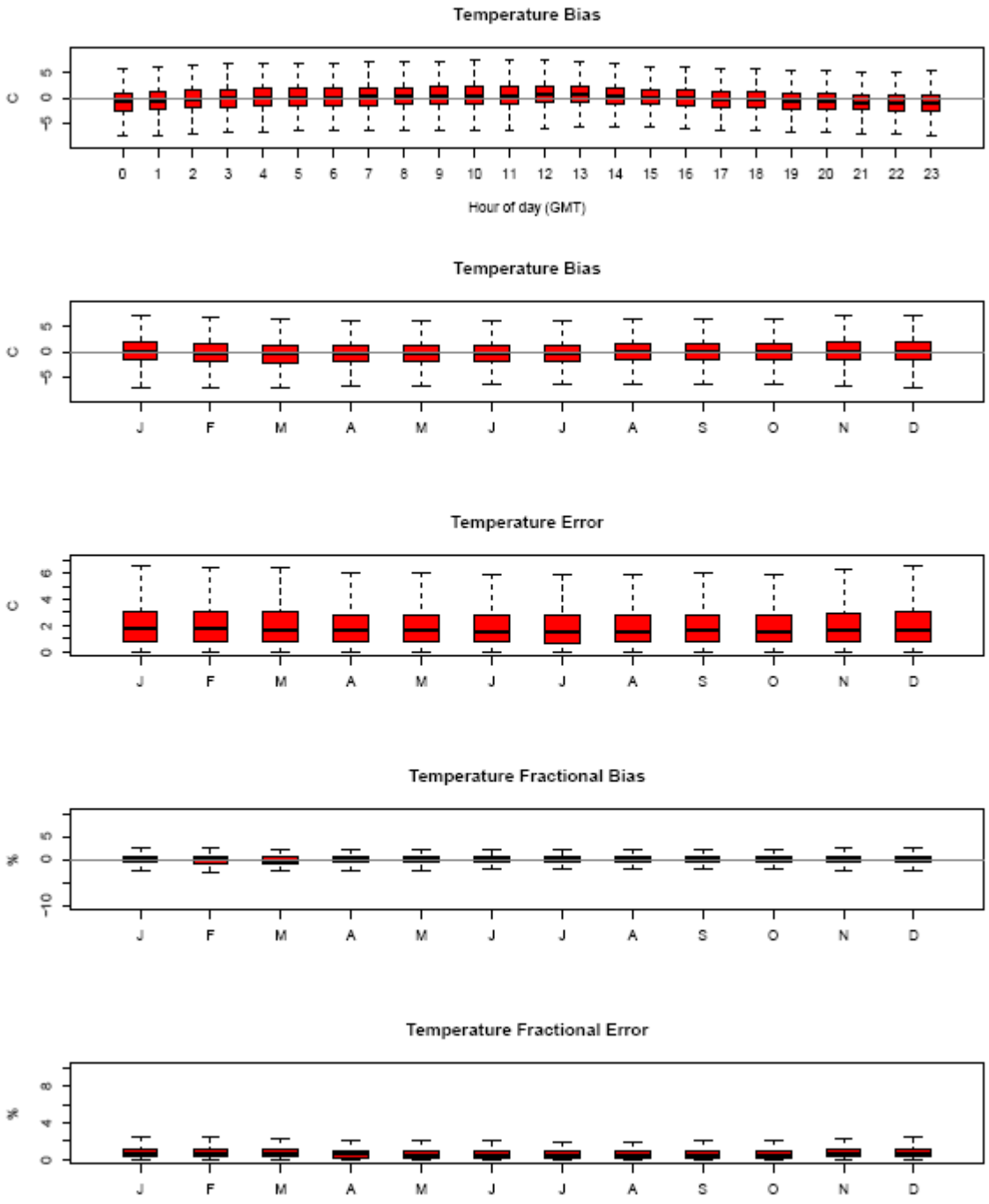

Figure 3.2.2. Distribution of hourly bias by hour and hourly bias, error, fractional bias, and fractional error by month. Metrics shown for 36US domain.

3.3 Mixing Ratio

Water mixing ratio estimates are compared to surface based measurements made at NCAR's ds472 network monitors for the 12US (Figure 3.3.1) and 36US (Figure 3.3.2) domains. Outliers are not plotted on these box plots to emphasize predominant features in model performance. The outer edges of the box represent the 25th and 75th percentiles and the edges of the whiskers represent the 10th and 90th percentiles of the distributions. These plots show the entire distribution of hourly bias (model-observation) by month and by hour of the day. In addition, these Figures show other metrics including mean error, fractional bias, and fractional error.

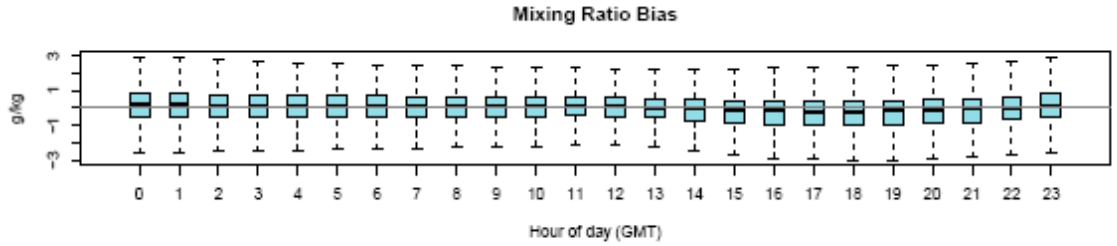

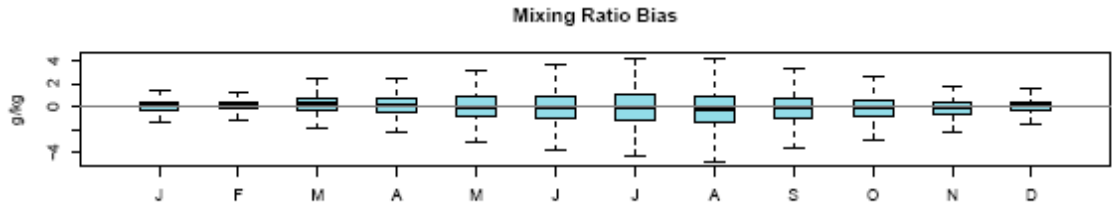

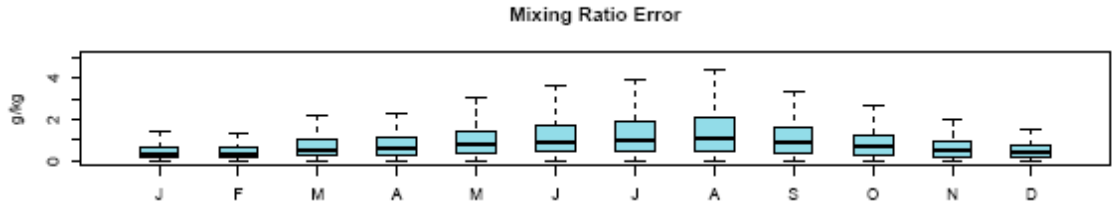

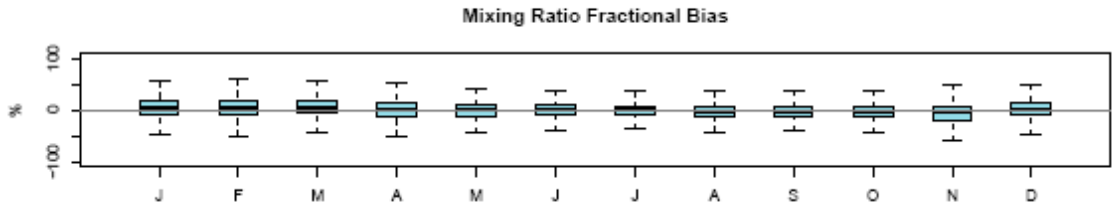

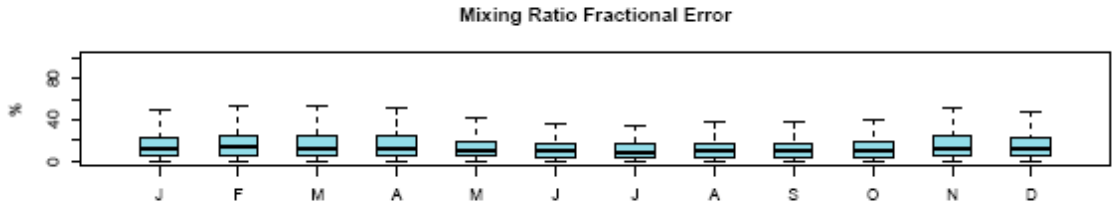

Figure 3.3.1. Distribution of hourly bias by hour and hourly bias, error, fractional bias, and fractional error by month. Metrics shown for 12US domain.

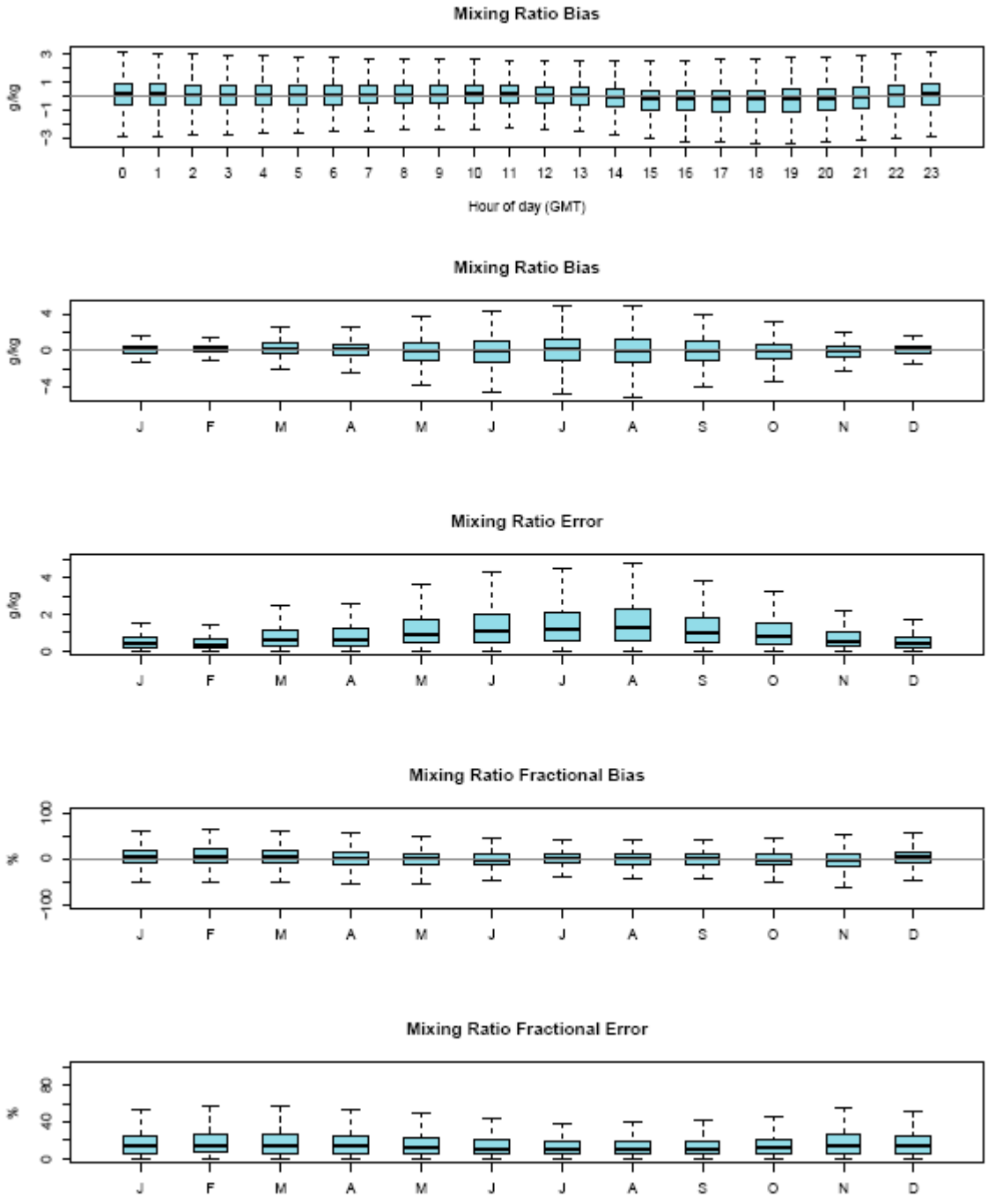

Figure 3.3.2. Distribution of hourly bias by hour and hourly bias, error, fractional bias, and fractional error by month. Metrics shown for 36US domain.

3.4 Solar Radiation

Photosynthetically activated radiation (PAR) is a fraction of shortwave downward radiation and is an important input for the biogenic emissions model for estimating isoprene (Carlton and Baker, 2011). Isoprene emissions are important for regional ozone chemistry and play a role in secondary organic aerosol formation. Radiation performance evaluation also gives an indirect assessment of how well the model captures cloud formation during daylight hours.

Shortwave downward radiation estimates are compared to surface based measurements made at SURFRAD and ISIS network monitors for the 12US domain (Figure 3.4.1) and 36US domain (Figure 3.4.2). Outliers are not plotted on these box plots to emphasize predominant features in model performance. The outer edges of the box represent the 25th and 75th percentiles and the edges of the whiskers represent the 10th and 90th percentiles of the distributions. These plots show the entire distribution of hourly bias (model-observation) by month and by hour of the day.

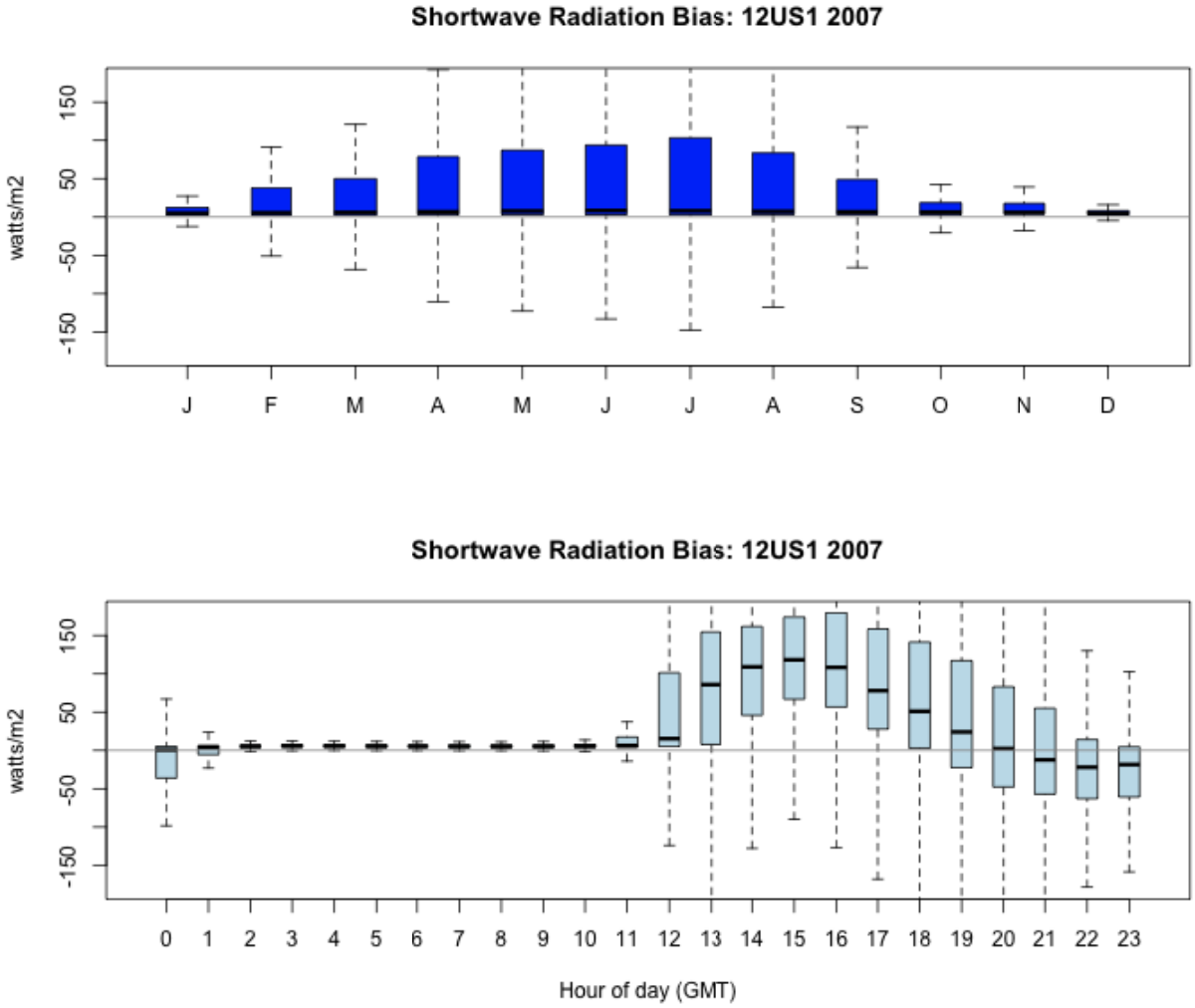

Table 3.4.1. Distribution of hourly bias by month (top) and hour of the day (bottom). Metrics shown for 12US domain.

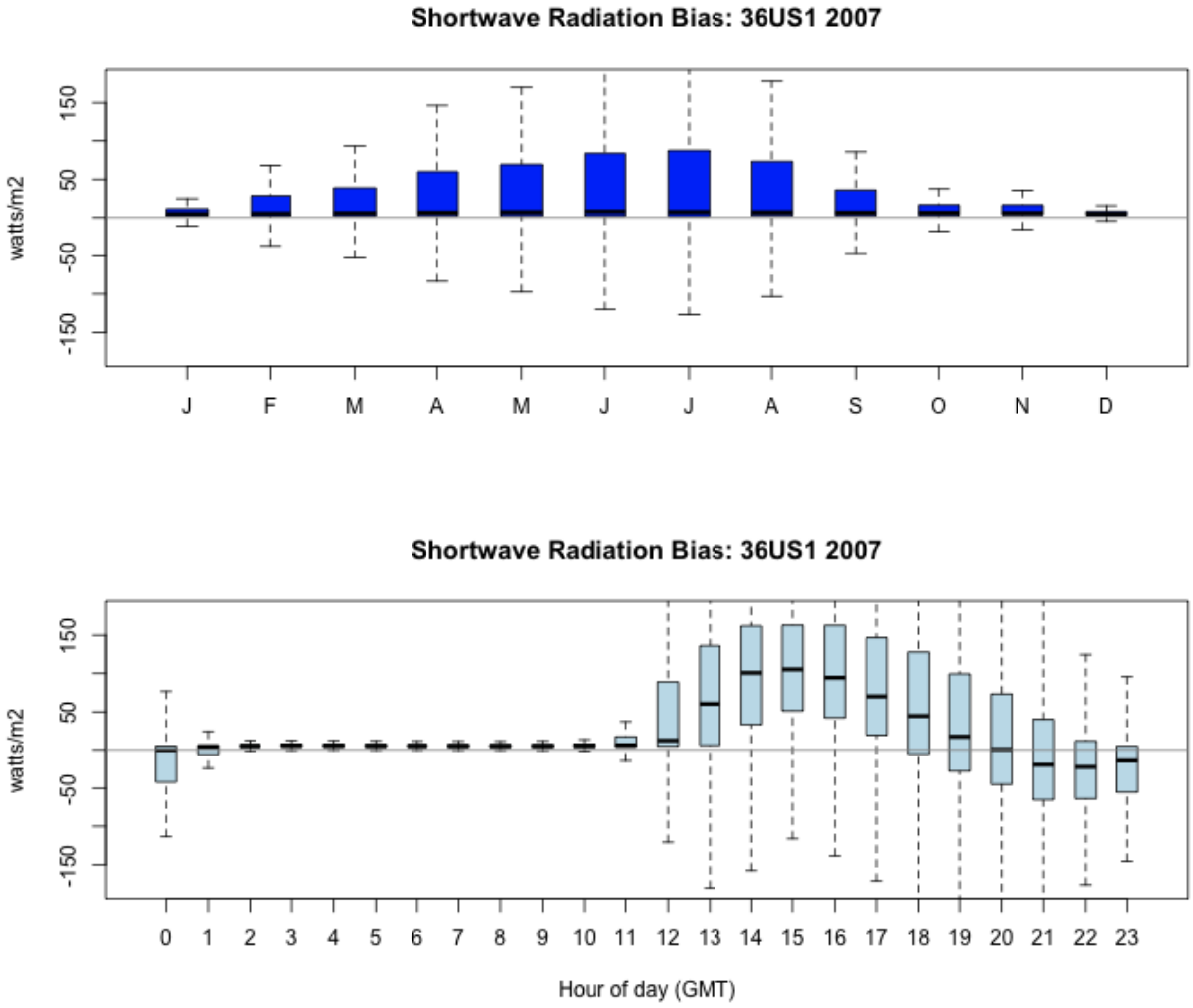

Table 3.4.2. Distribution of hourly bias by month (top) and hour of the day (bottom). Metrics shown for 36US domain.

3.5 Precipitation

Monthly total rainfall is plotted for each grid cell to assess how well the model captures the spatial variability and magnitude of convective and non-convective rainfall events. Rainfall is only estimated by the PRISM analysis inside the continental United States. This means comparisons of monthly total rainfall offshore and in Canada and Mexico are not possible with this product. WRF rainfall estimates by month are shown for all grid cells in the domain. Monthly total estimates are shown for the 12US domain from Figure 3.5.1 to Figure 3.5.4 and for the 36US domain from Figure 3.5.5 to Figure 3.5.8.

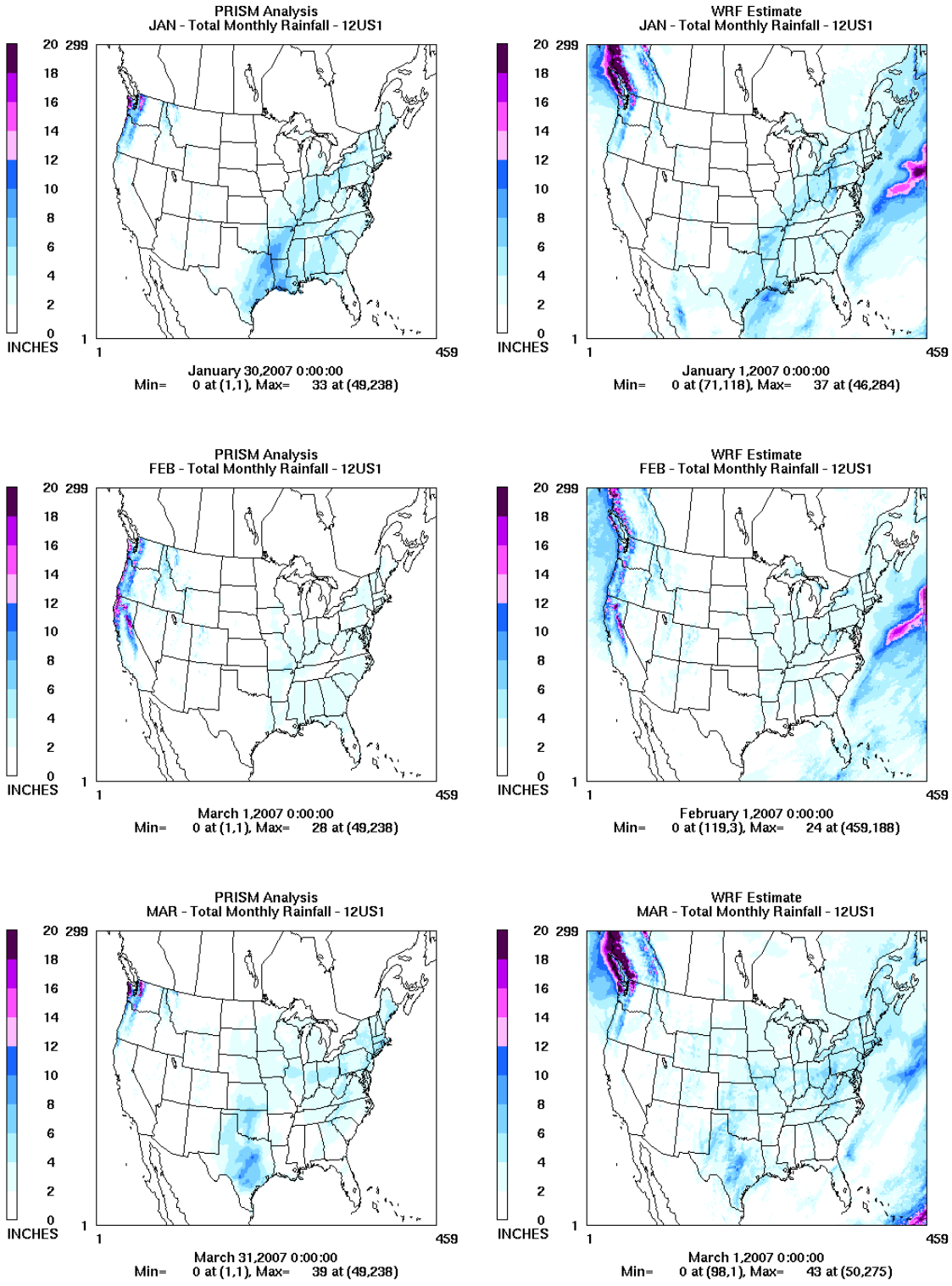

Figure 3.5.1 PRISM analysis (left) and WRF (right) estimated monthly total rainfall for January, February, and March.

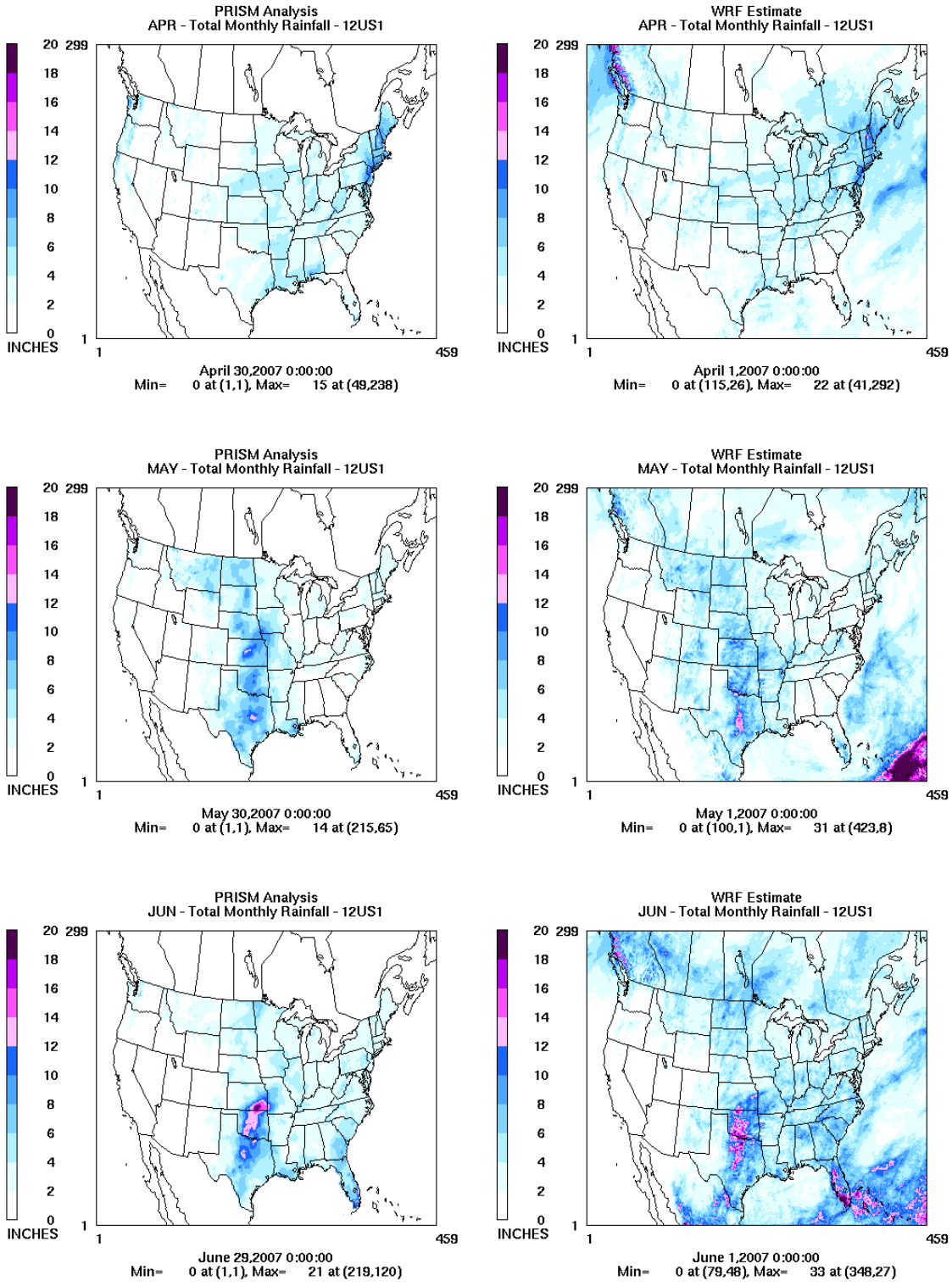

Figure 3.5.2 PRISM analysis (left) and WRF (right) estimated monthly total rainfall for April, May, and June.

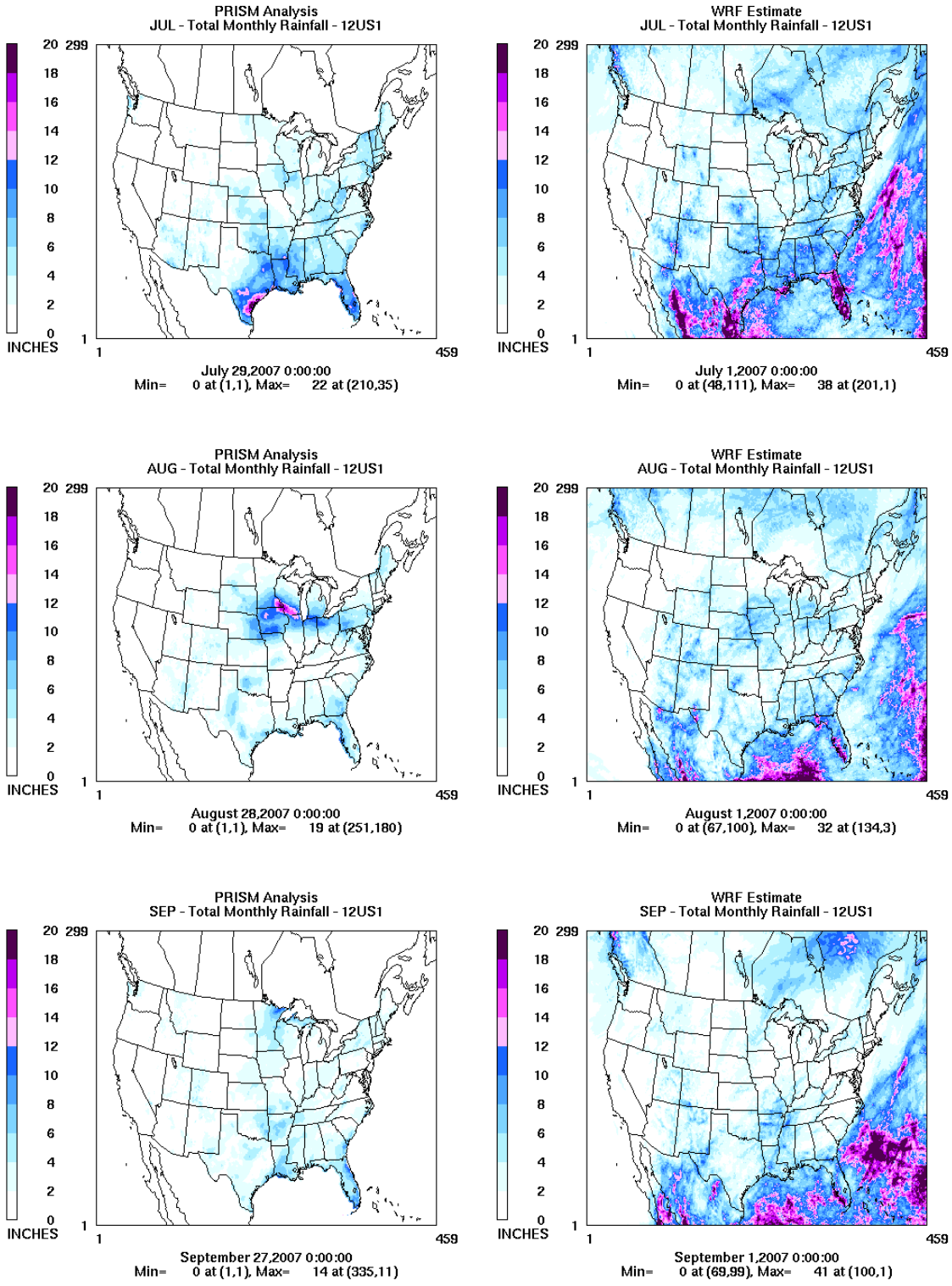

Figure 3.5.3 PRISM analysis (left) and WRF (right) estimated monthly total rainfall for July, August, and September.

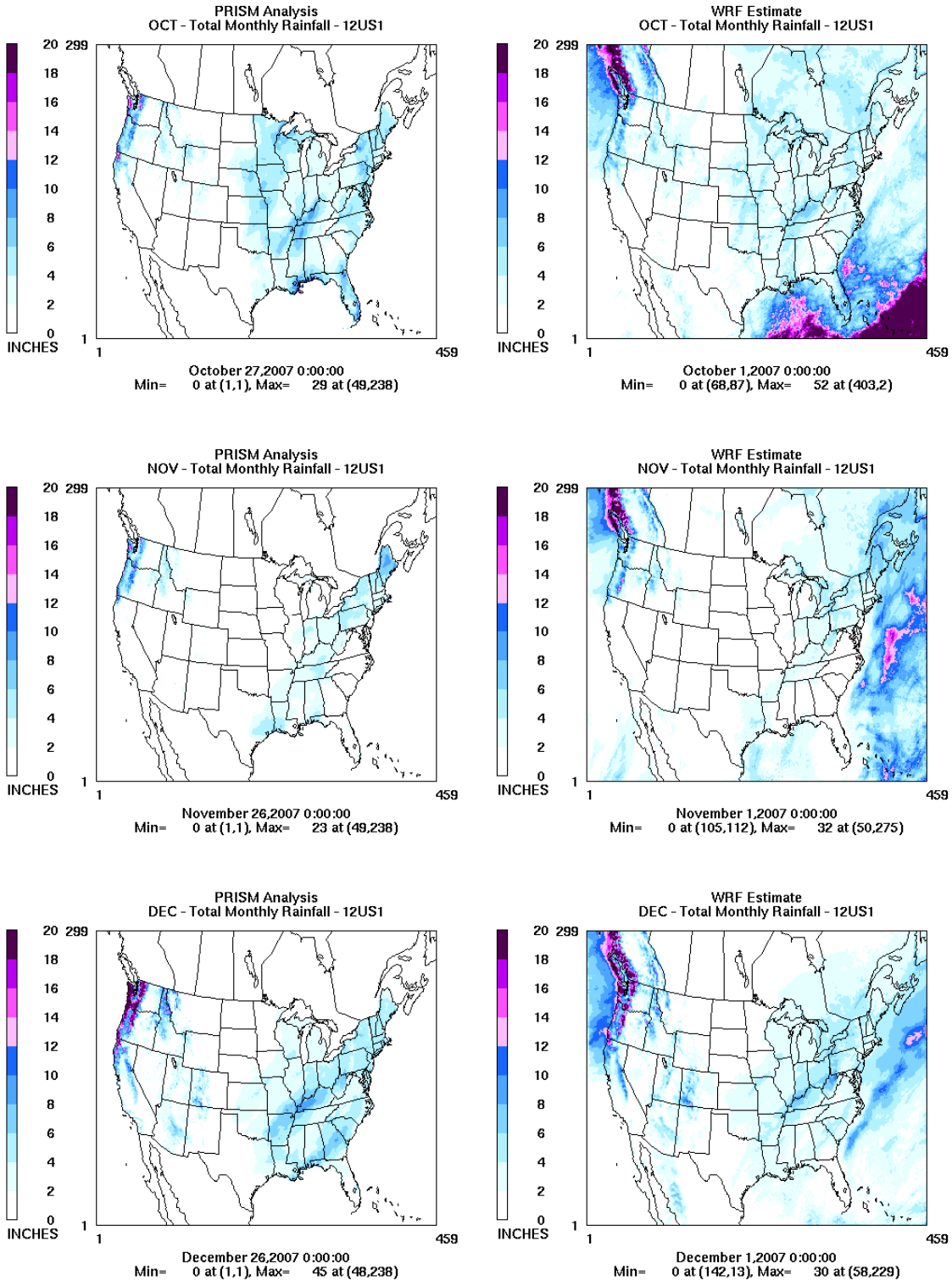

Figure 3.5.4 PRISM analysis (left) and WRF (right) estimated monthly total rainfall for October, November, and December.

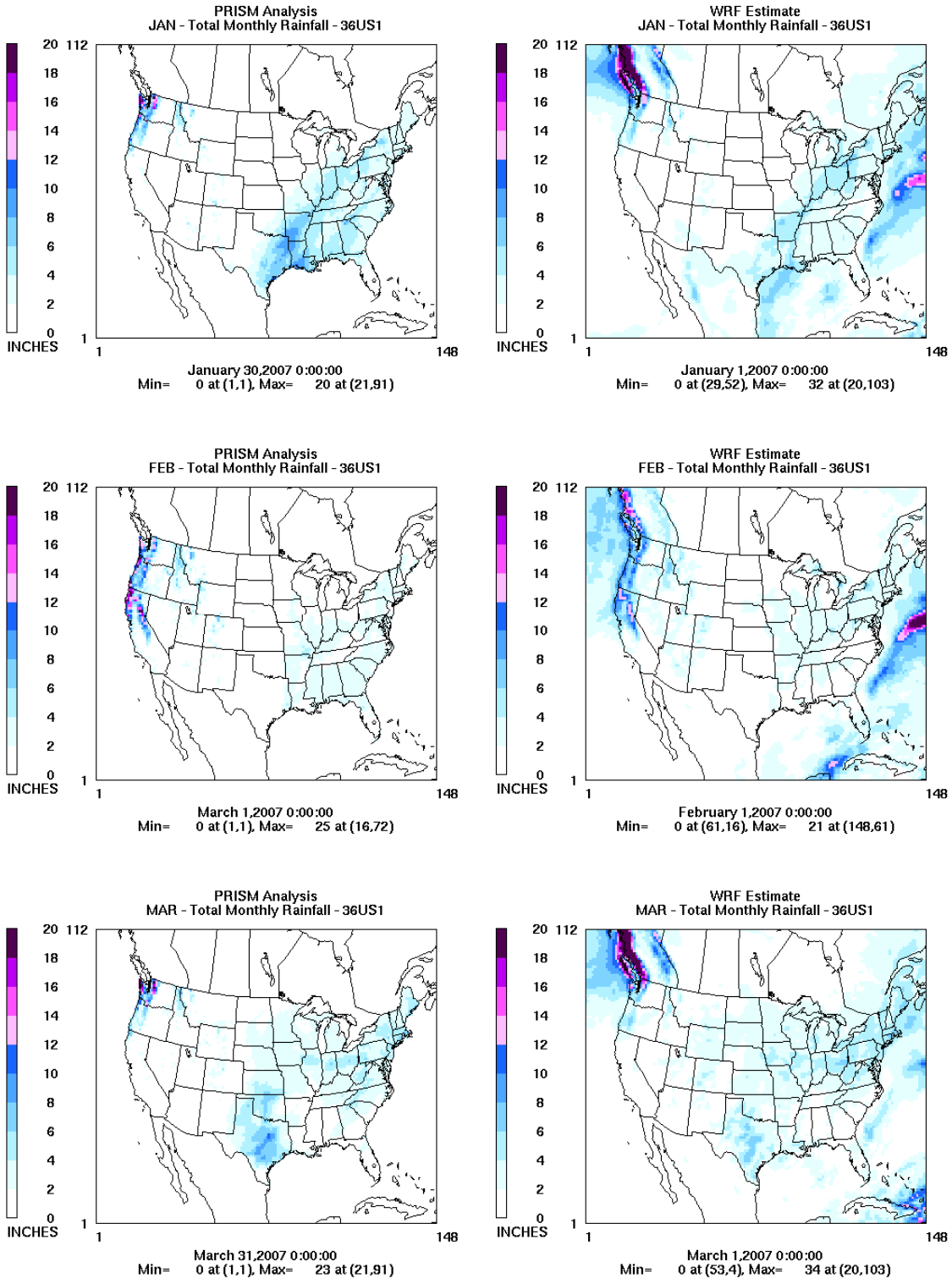

Figure 3.5.5 PRISM analysis (left) and WRF (right) estimated monthly total rainfall for January, February, and March.

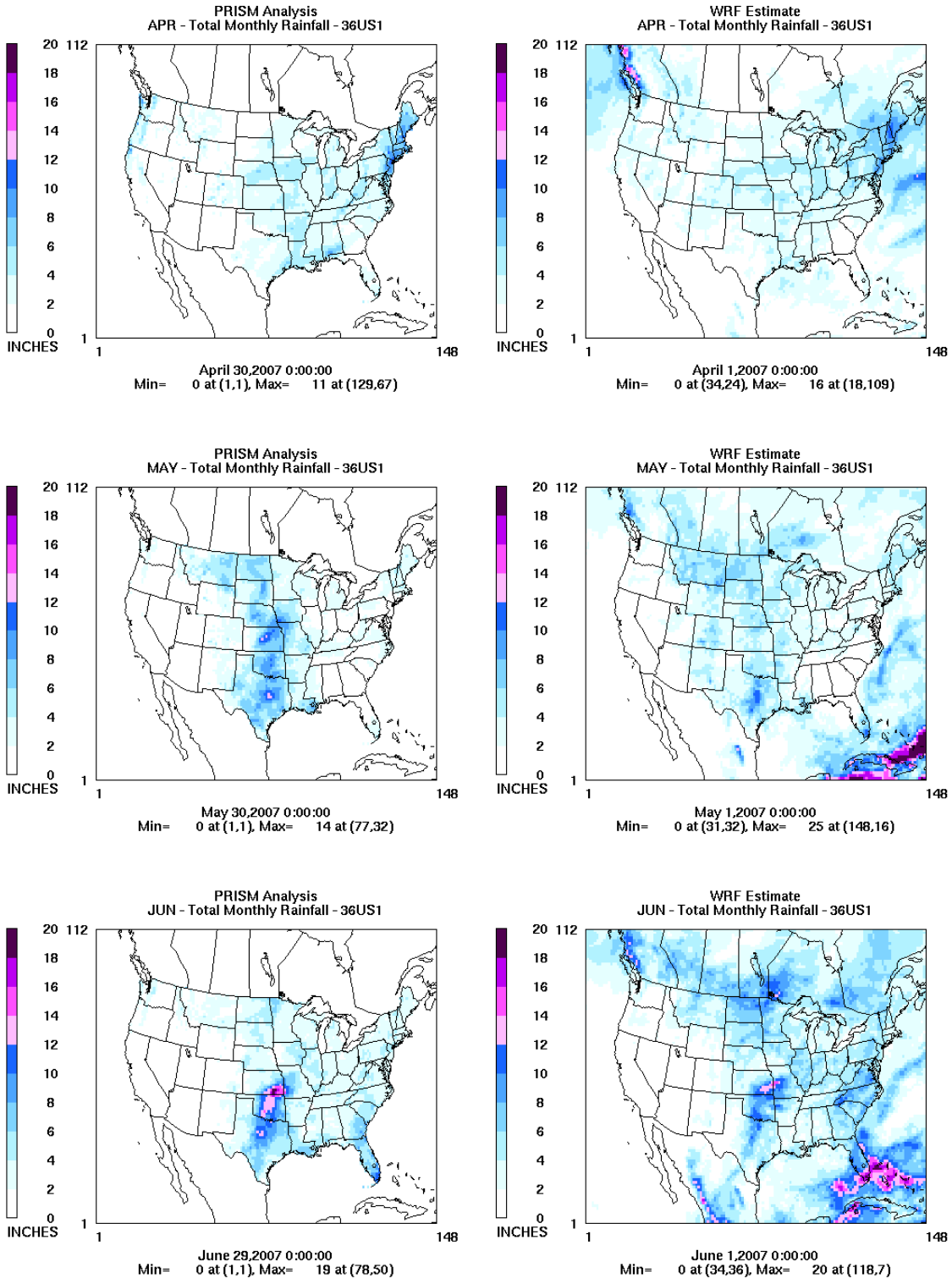

Figure 3.5.6 PRISM analysis (left) and WRF (right) estimated monthly total rainfall for April, May, and June.

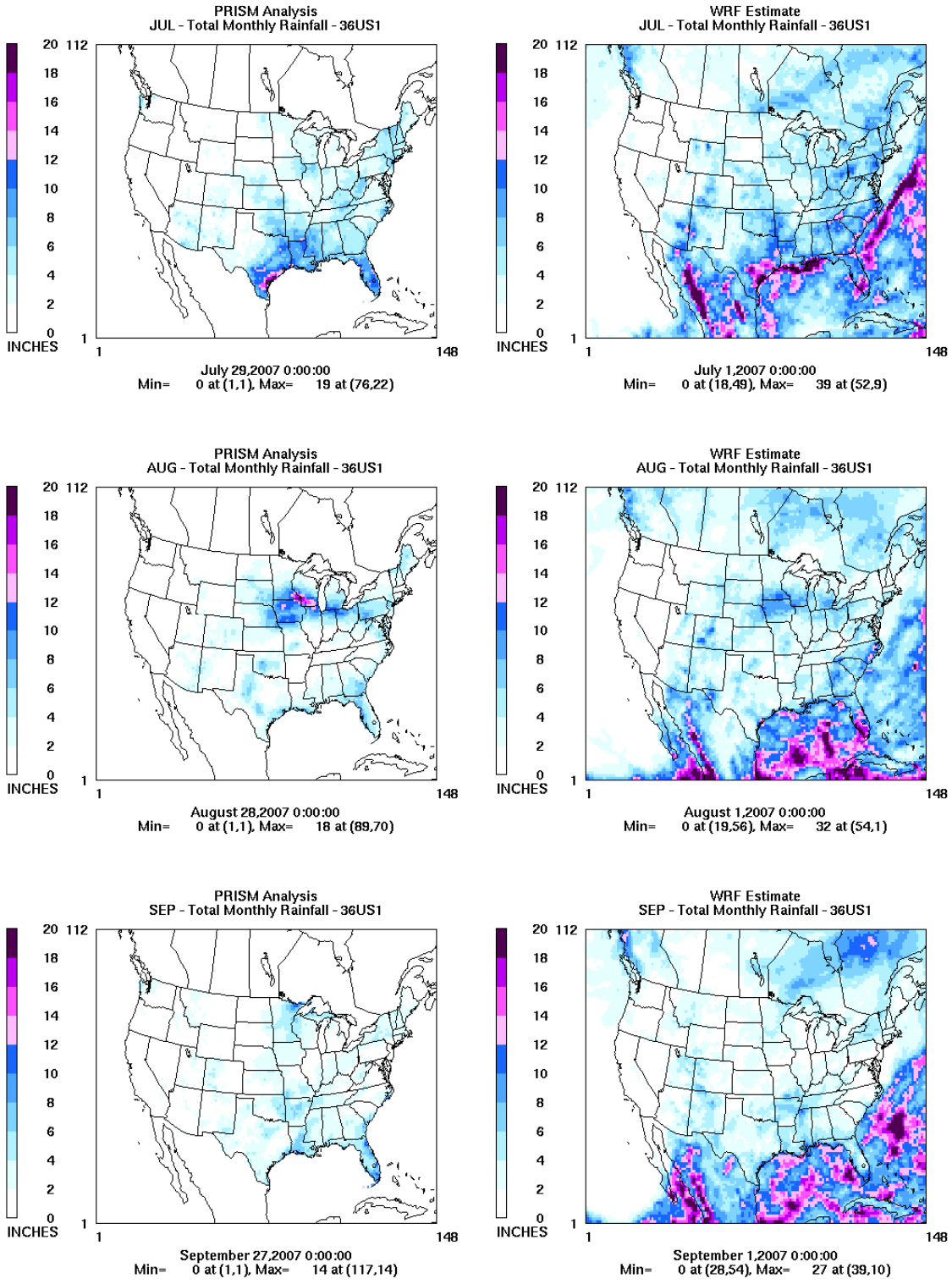

Figure 3.5.7 PRISM analysis (left) and WRF (right) estimated monthly total rainfall for July, August, and September.

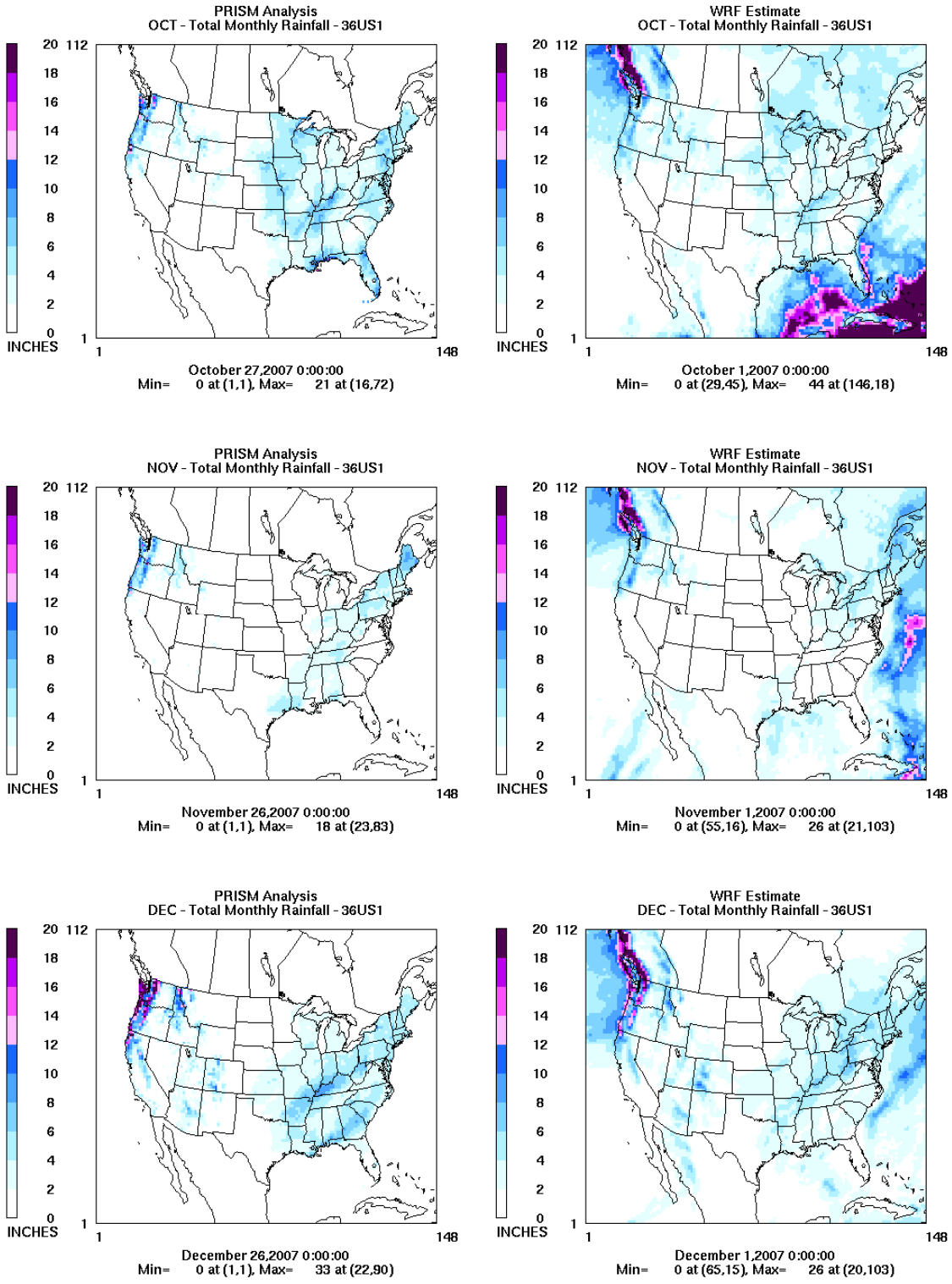

Figure 3.5.8 PRISM analysis (left) and WRF (right) estimated monthly total rainfall for October, November, and December.

3.6 Maximum Predicted PBL

Maximum planetary boundary layer heights are plotted for each grid cell by month for the 12US domain (Figure 3.6.1) and 36US domain (Figure 3.6.2). These plots are generated to help assess whether unrealistic stratospheric intrusion may occur in any of the simulated months.

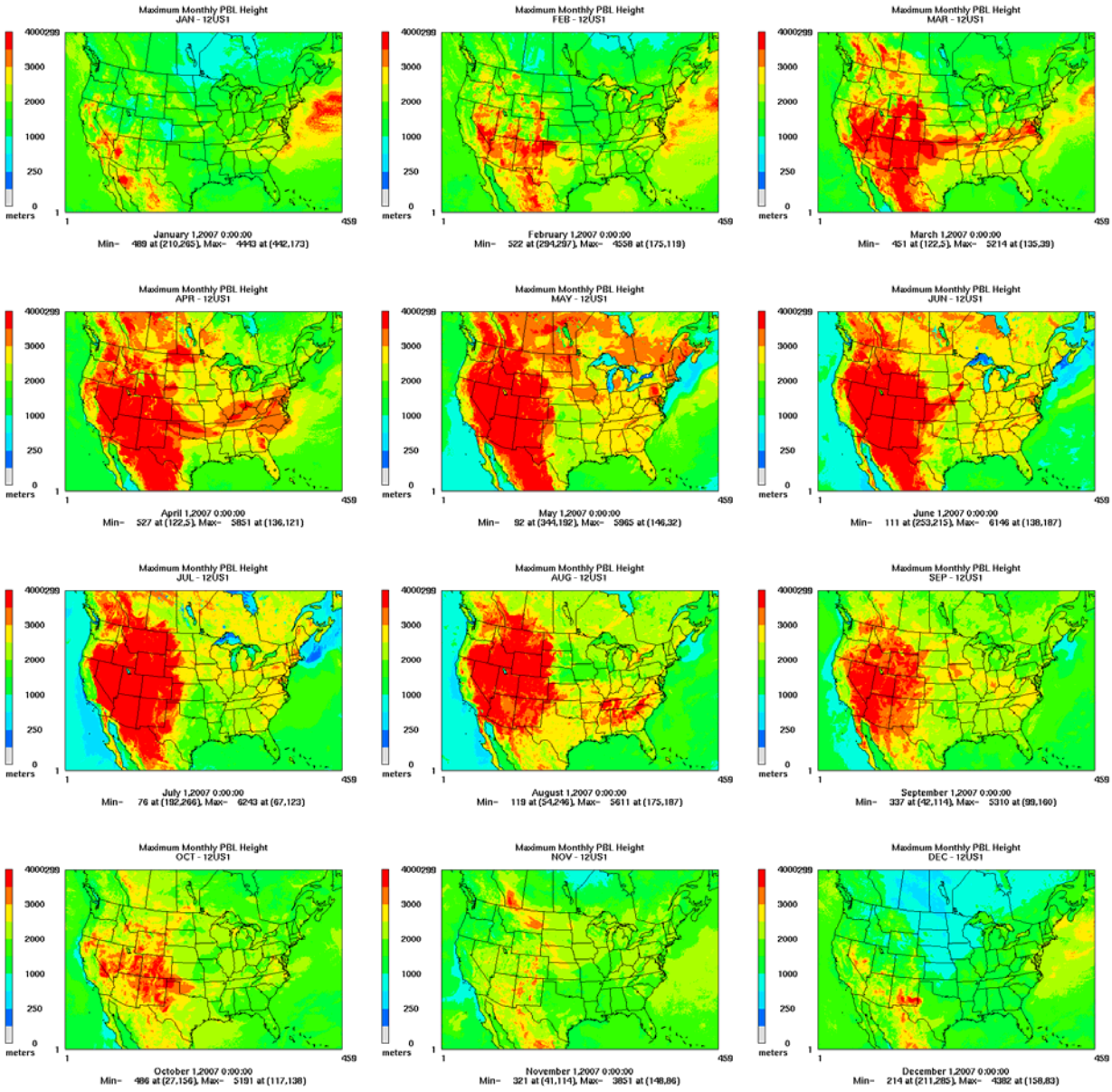

Table 3.6.1. Monthly maximum estimated planetary boundary layer heights estimated by WRF. Plots show 12US domain.

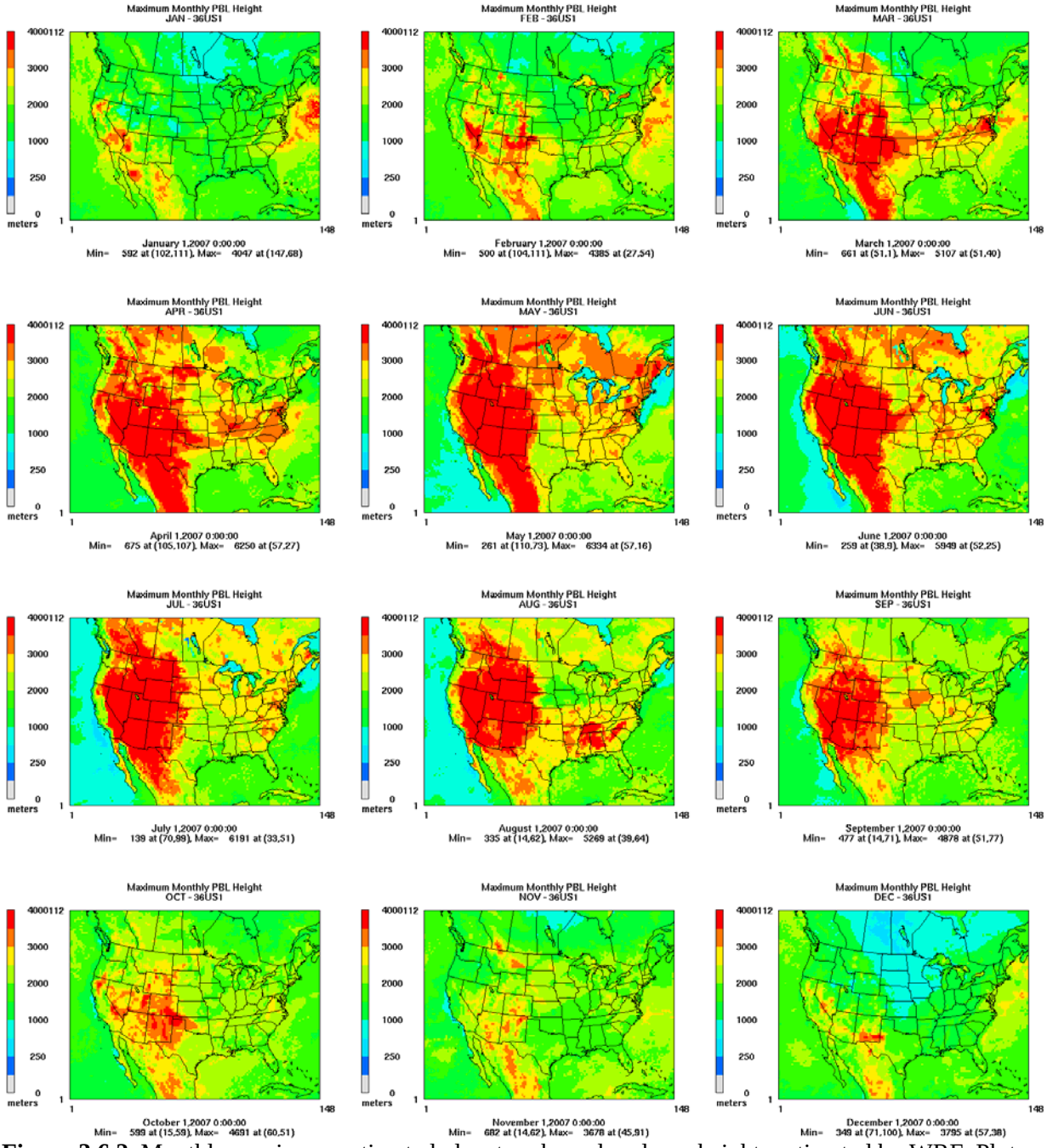

Figure 3.6.2. Monthly maximum estimated planetary boundary layer heights estimated by WRF. Plots show 36US domain.

4 REFERENCES

Boylan, J.W., Russell, A.G., 2006. PM and light extinction model performance metrics, goals, and criteria for three-dimensional air quality models. Atmospheric Environment 40, 4946-4959.

Carlton, A.G., Baker, K.R., 2011. Photochemical Modeling of the Ozark Isoprene Volcano: MEGAN, BEIS, and Their Impacts on Air Quality Predictions. Environmental Science & Technology 45, 4438-4445.

ENVIRON, 2008. User's Guide Comprehensive Air Quality Model with Extensions. ENVIRON International Corporation, Novato.

Gilliam, R.C., Pleim, J.E., 2010. Performance Assessment of New Land Surface and Planetary Boundary Layer Physics in the WRF-ARW. Journal of Applied Meteorology and Climatology 49, 760-774.

Otte, T.L., Pleim, J.E., 2010. The Meteorology-Chemistry Interface Processor (MCIP) for the CMAQ modeling system: updates through MCIPv3.4.1. Geoscientific Model Development 3, 243-256.

Skamarock, W.C., Klemp, J.B., Dudhia, J., Gill, D.O., Barker, D.M., Duda, M.G., Huang, X., Wang, W., Powers, J.G., 2008. A Description of the Advanced Research WRF Version 3.

APPPENDIX A

Climatic Charts for 2007

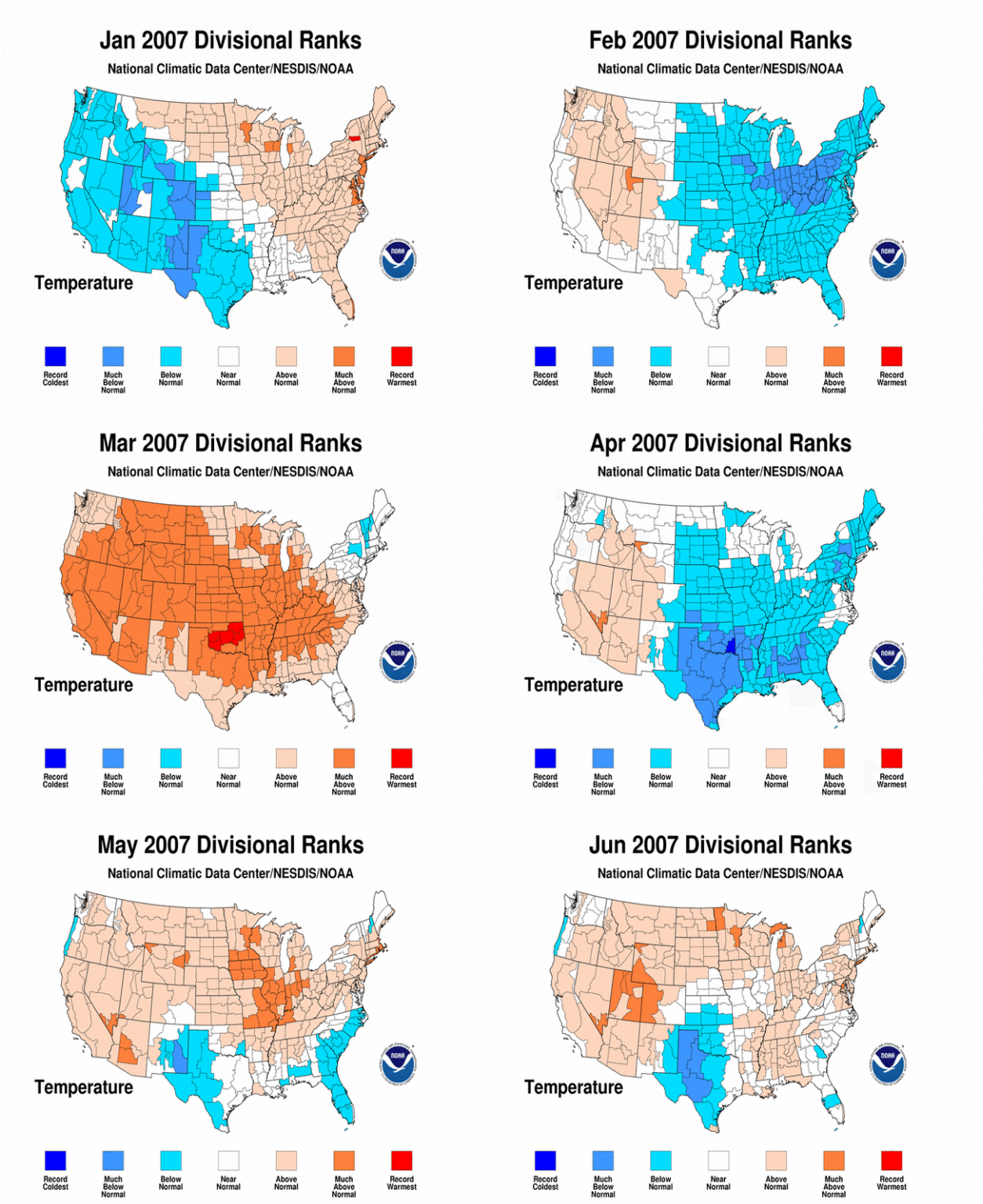

Figure A.1 Climatic rainfall rankings by climate division: January to June 2007.

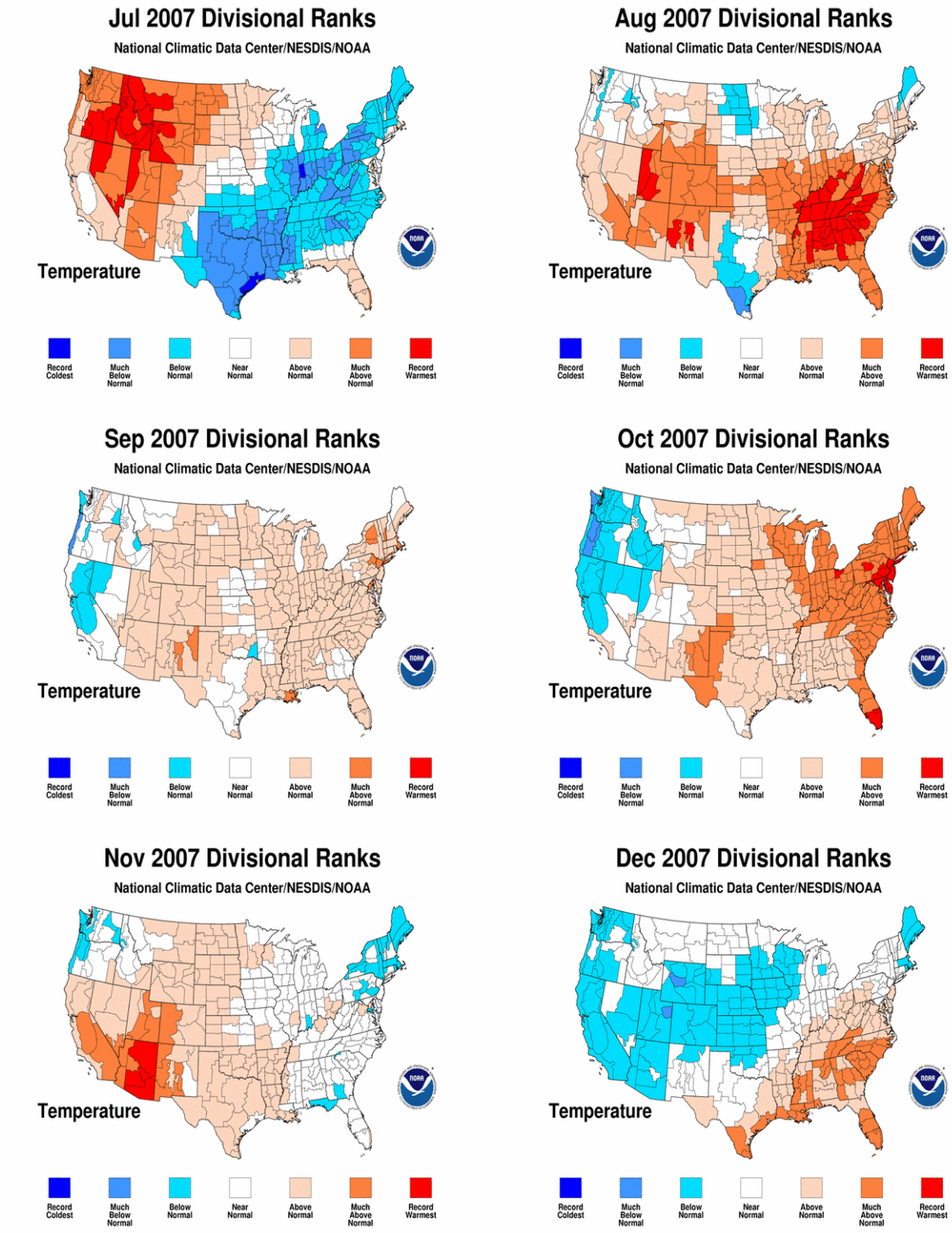

Figure A.2 Climatic rainfall rankings by climate division: July to December 2007.

United States
Environmental Protection
Agency

Office of Air Quality Planning and Standards
Air Quality Assessment Division
Research Triangle Park, NC

Publication No. EPA-454/R-11-007
October 2011